# Excitability of the Squid Giant Axon Revisited

JOHN R. CLAY
*Laboratory of Neurophysiology, National Institute of Neurological Disorders and Stroke, National Institutes of Health, Bethesda, Maryland 20892; and the Marine Biological Laboratory, Woods Hole, Massachusetts 02543*

**Clay, John R.** Excitability of the squid giant axon revisited. *J. Neurophysiol.* 80: 903–913, 1998. The electrical properties of the giant axon from the common squid *Loligo pealei* have been reexamined. The primary motivation for this work was the observation that the refractoriness of the axon was significantly greater than the predictions of the standard model of nerve excitability. In particular, the axon fired only once in response to a sustained, suprathreshold stimulus. Similarly, only a single action potential was observed in response to the first pulse of a train of 1-ms duration current pulses, when the pulses were separated in time by ~10 ms. The axon was refractory to all subsequent pulses in the train. The underlying mechanisms for these results concern both the sodium and potassium ion currents $I_{Na}$ and $I_K$. Specifically, $Na^+$ channel activation has long been known to be coupled to inactivation during a depolarizing voltage-clamp step. This feature appears to be required to simulate the pulse train results in a revised model of nerve excitability. Moreover, the activation curve for $I_K$ has a significantly steeper voltage dependence, especially near its threshold (approximately −60 mV), than in the standard model, which contributes to reduced excitability, and the fully activated current-voltage relation for $I_K$ has a nonlinear, rather than a linear, dependence on driving force. An additional aspect of the revised model is accumulation/depeletion of $K^+$ in the space between the axon and the glial cells surrounding the axon, which is significant even during a single action potential and which can account for the 15–20 mV difference between the potassium equilibrium potential $E_K$ and the maximum afterhyperpolarization of the action potential. The modifications in $I_K$ can also account for the shape of voltage changes near the foot of the action potential.

## INTRODUCTION

In their classic work over forty years, ago Hodgkin and Huxley (1952a–d) described a model of the action potential of the squid giant axon that was based on their measurements of ion currents in this preparation. The model has been so widely accepted as a paradigm for excitable membranes that its appropriateness for the giant axon itself has generally not been questioned. The main finding in this report is that the model does not provide a good description of many electrophysiological properties of the axon, in particular the refractory behavior of the preparation in response either to sustained or periodic current pulse stimulation. The modifications of the model that are sufficient to explain these results concern both the sodium and potassium ion currents $I_{Na}$ and $I_K$. Measurements of $I_{Na}$ kinetics have long been known to be inadequately described by the Hodgkin and Huxley (1952d) model (hereafter refered to as the HH model) of $I_{Na}$ [the "$m^3h$" kinetics; a full description of the inadequacies of this model is provided by Patlak (1991)]. Specifically, $Na^+$ channel activation and inactivation kinetics are coupled (Bezanilla and Armstrong 1977), as opposed to the HH model in which these processes are independent of each other. This revised description of $I_{Na}$ kinetics has been fully implemented for squid giant axons by Vandenberg and Bezanilla (1991b). Their model of $I_{Na}$ is used in the simulations given below. The response of an axon to a train of brief duration depolarizing current pulses appears to require the revised $I_{Na}$ kinetics in simulations of these results.

The modifications in $I_K$ pertain primarily to its fully activated current-voltage relation, which has a nonlinear dependence on driving force, $(V - E_K)$. This result is well described by the Goldman, Hodgkin, and Katz (GHK) relation (Clay 1991; Binstock and Goldman 1971; Goldman 1943; Hodgkin and Katz 1949). [The fully activated current-voltage relation for the $Na^+$ channel is also well described by the GHK equation (Vandenberg and Bezanilla 1991a).] Determination of steady-state activation of $I_K$ by using this result rather than a linear dependence of the current-voltage relation on driving force yields an activation curve having a much steeper voltage dependence than the original HH model description of this parameter (Clay 1995), which contributes to a reduced excitability of the revised model relative to the HH model. Moreover, accumulation of potassium ions in the space between the axon membrane and the glial cells surrounding the axon [i.e., the Frankenhauser and Hodgkin (1956), or FH space] appears to be significantly greater than previously realized, even during a single action potential. A novel feature of this analysis is the observation that the glial cells appear to act not only as a diffusional barrier to ions leaving the axon, but also as an uptake mechanism for potassium ions, especially when the $K^+$ concentration in the FH space is only slightly higher than in the external solution. The GHK voltage dependence of the fully activated current-voltage relation together with the accumulation/depletion process in the FH space can account for the shape of the action potential during the latter part of its repolarization phase. The revisions in $I_K$ also account for the marked increase in the amplitude of the afterhyperpolarization of the action potential after removal of extracellular potassium ions.

## METHODS

Experiments were performed on common North Atlantic squid (*Loligo pealei*) by using standard axial wire current- and voltage-clamp techniques described elsewhere (Clay and Shlesinger 1983; French and Wells 1977). Measurements of excitability in current-clamp conditions were carried out either with the axoplasm in place or with an intracellular perfusate consisting of the following (in mM): 250 K glutatmate, 30 Na glutamate, 25 $K_2HPO_4$, and 350 sucrose, pH 7.2 (standard perfusate); in some experiments the 25 $K_2HPO_4$ in this solution was replaced by 50 KF. The extracellular solution for these results was filtered seawater, except for Fig. 6, *A*

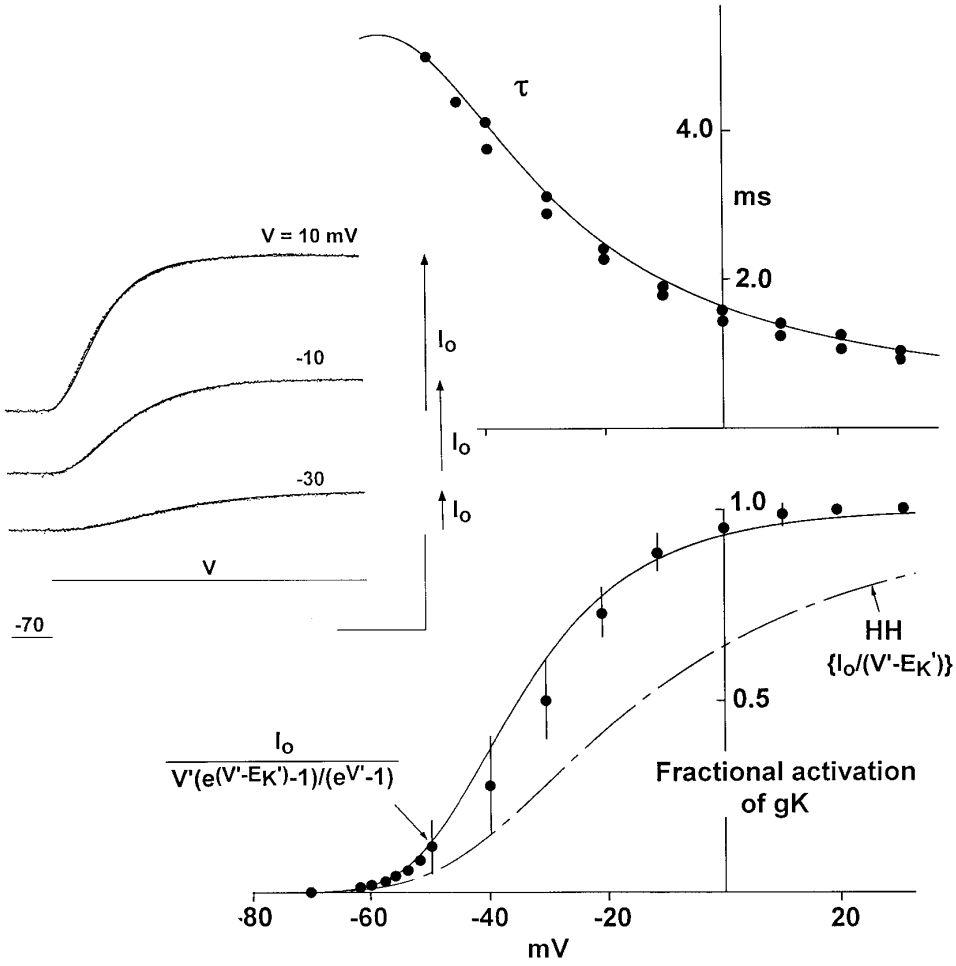


FIG. 1. Revisions in the model of $I_K$. *Inset*: currents elicited by voltage steps to the potentials indicated in tetrodotoxin–artificial seawater (TTX–ASW). $T$ = 8°C. Scales represent 5 ms and 1 mA·cm$^{-2}$, respectively. Superimposed on each record is a fit, by eye, of the expression $[1 - \exp(-t/\tau)]^4$, where $\tau$ = 3.8, 2.3, and 2.0 ms, respectively, for $V$ = −30, −10, and + 10 mV. Holding potential = −70 mV. The currents at the end of these steps are represented by the arrows labeled $I_O$. The time constants obtained by this procedure from 2 different preparations are given in the *top panel*. The activation curve for $I_K$ was obtained by scaling the $I_O$ results by the Goldman-Hodgkin-Katz (GHK) equation as described in RESULTS and as indicated in the *bottom panel* ($V'$ = V/24). Each result labeled with a filled circle represents mean ± SD ($n$ = 4). The solid line corresponds to $n_\infty^4 = [\alpha_n/(\alpha_n + \beta_n)]^4$, with $\alpha_n = -0.01(V + 50)/\{\exp[-0.1(V + 50)] - 1\}$ and $\beta_n = 0.1\exp[-(V + 60)/25]$. The dashed line represents $n_\infty^4$ in the Hodgkin and Huxley (1952d) model (HH model) that is the same as in the revised model but with $\beta_n = 0.125\exp[-(V + 60)/80]$ rather than $\beta_n = 0.1\exp[-(V + 60)/25]$. (Note that changing the ''80'' in the denominator of the exponential term in the original expression for $\beta_n$ in the HH model to ''25'' is sufficient to significantly steepen the voltage dependence of the $I_K$ activation curve.)

and *B*, for which artificial seawater (ASW) and potassium-free artificial seawater (0 $K^+$ SW) was used, respectively. The former consisted of the following (in mM): 430 NaCl, 50 $MgCl_2$, 10 $CaCl_2$, 10 KCl, and 10 tris(hydroxymethyl)aminoethane (Tris)-HCl, pH 7.2; the latter consisted of the following (in mM): 440 NaCl, 50 $MgCl_2$, 10 $CaCl_2$, and 10 Tris-HCl. The records of $I_K$ in Fig. 1 were obtained with ASW to which 1 $\mu$M tetrodotoxin (TTX; Sigma, St. Louis, MO) was added and an intracellular perfusate consisting of 250 mM K glutamate, 50 mM KF, and 400 mM sucrose. The latter also was used for the experiment in Fig. 2, along with TTX-0 $K^+$ SW as the extracellular solution. The liquid junction potentials were <3 mV. The results given in this paper have not been corrected for these relatively small offsets. Unless otherwise stated, the temperature used in these experiments was 8°C. It was maintained constant to within 0.1°C in any single experiment by a Peltier device located within the experimental chamber.

Voltage- and current-clamp recordings were made with the aid of custom designed stimulus and data acquisition software (Alembic Software, Montreal, Quebec, Canada). Except for the records in Fig. 6, which are photographs of oscilloscope traces, all experimental traces shown here were generated with the aid of a software plot routine. Computer simulations of membrane excitability were carried out with a fourth order Runge-Kutta iteration routine implemented in FORTRAN with a step size of 1 $\mu$s for the HH and revised models of membrane excitability, respectively, which are given in the APPENDIX.

## RESULTS

Some of the discrepancies between the HH model and squid axon behavior have been previously noted (Adelman and Fitzhugh 1975; Hodgkin 1964). These and other results are given below after a description of the underlying ionic currents.

### *Revised model of $I_{Na}$*

As noted above, the Vandenberg and Bezanilla (1991b) kinetic description of $I_{Na}$ was used in the simulations in this report. Their model (which is similar to that originally proposed by Armstrong and Bezanilla 1977) is given by

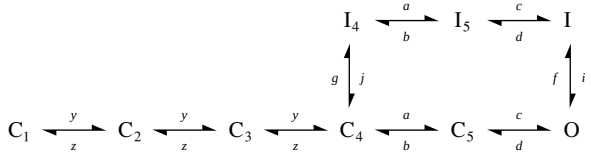


where $C_i$, $i$ = 1, 2...5, are closed states; O is the open state; and I, $I_4$, and $I_5$ are inactivated states of the channel. The various rate parameters of the model ($a$, $b$, $c$, $d$, $f$, $g$, $i$, $y$, and $z$) are given in the APPENDIX and have been modified as follows. The model as given in Vandenberg and Bezanilla (1991b) corresponds to conditions in which the external solution does not contain divalent cations. Seawater contains 50 mM $Mg^{2+}$ and 10 mM $Ca^{2+}$, conditions that shift all of the $I_{Na}$ kinetics parameters ~10 mV rightward along the

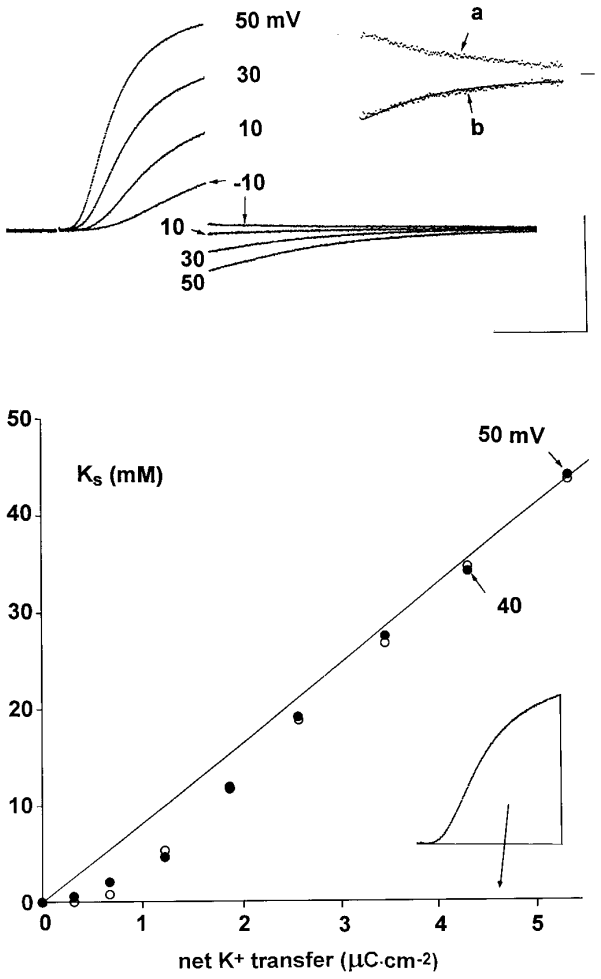


FIG. 2. $K^+$ accumulation. Records in *top panel* were elicited by 3-ms duration steps to the potentials indicated followed by a return to the holding potential (−90 mV). Same conditions as in Fig. 1 except that 0 $K_O$ seawater was used. Scales represent 2 ms and 1 mA·cm$^{-2}$, respectively. Record labeled ''a'' in the *top inset* is the −10 mV tail current record shown on expanded vertical scale and a reduced horizontal scale. This result is inverted and superimposed on the 50 mV tail current (with appropriate scaling of current amplitude). The composite result is labeled ''b.'' The effective potassium ion concentration in the periaxonal space ($K_S$) at the end of each depolarizing step was obtained from the current at the end of the step ($I_1$) and at the beginning of the tail current ($I_2$) and the equation $I_K = \delta V/24[K_i \exp(V/24) - K_S]/[\exp(V/24) - 1]$, where $\delta$ is a constant that is proportional to channel activation. ($K_i$ = 0.3 M.) Specifically, $I_1 = \delta V_1/24[0.3 \exp(V_1/24) - K_S]/[\exp(V_1/24) - 1]$, with a similar equation relating $I_2$ and $V_2$, where $V_1$ is the voltage of the depolarizing step and $V_2$ is the holding potential (−90 mV). These are 2 equations with 2 unknowns, i.e., $\delta$ and $K_S$. The results for $K_S$ are represented by the ordinate. The results for $\delta$ (not shown) were as expected, based on the activation curve in Fig. 1. The abscissa represents the integral of the current elicited by the depolarizing step as indicated, schematically, in the *inset* in the *bottom right-hand corner*. Filled circles are experimental points; open symbols are results of the analysis described in the text.

voltage axis, as shown in Vandenberg and Bezanilla (1991a). Consequently, all of the rate parameters in the above model have been rightward shifted by 10 mV (see APPENDIX). Furthermore, Vandenberg and Bezanilla (1991a,b) carried out their experiments at 5°C, whereas the experiments in this study were performed at 8°C. Consequently, all of the rate parameters in the $I_{Na}$ model have been multiplied by a factor of 1.3, which adequately accounts for the effect of changing the temperature from 5 to 8°C (unpublished results).

The second aspect of the $I_{Na}$ model concerns the fully activated current-voltage relation for the $Na^+$ channel, which is well described by the Goldman-Hodgkin-Katz (GHK) equation (Goldman 1943; Hodgkin and Katz 1949; Vandenberg and Bezanilla 1991a), i.e.

$$I_{Na} = g_{Na} V \{\exp[q(V - E_{Na})/kT] - 1\}/[\exp(qV/kT) - 1] \quad (1)$$

where $g_{Na}$ is the limiting slope conductance ($V \rightarrow \infty$), $q$ is the unit electronic charge, $k$ is the Boltzmann constant, and $T$ is absolute temperature, with $kT/q$ = 24.1 mV at $T$ = 8°C (approximated by 24 mV hereafter), and $E_{Na}$ is the sodium ion equilibrium potential. [The expression $kT/q$ has more traditionally been given as $RT/F$, where $R$ is the universal gas constant and $F$ is the Faraday. Note that $R/F = k/q$.] *Equation 1* is modified by external divalent cation blockade of the $Na^+$ channel (Vandenberg and Bezanilla 1991b; Yamamoto et al. 1984), i.e., $I_{Na} \sim 1/(1 + [B]/K_d(0) \exp(-zdqV/kT))$, where $[B]$ is the divalent cation concentration, $K_d(0)$ is the dissociation constant of blockade at 0 mV, $z$ is the valence of the blocking ion, and $d$ is the fraction of the electric field sensed by the blocker. For 50 mM $Mg^{+2}$ and 10 mM $Ca^{2+}$ in the external solution, $[B]$ = 60 mM, $d$ = 0.19 mM, and $K_d(0)$ = 150 mM. Consequently, $I_{Na}$ in this analysis is given by

$$I_{Na} = g_{Na} P_O V \{\exp[(V - E_{Na})/24] - 1\}/\{[\exp(V/24) - 1] \times [1 + 0.4 \exp(-0.38V/24)]\}, \quad (2)$$

where $P_O$ is the probability that the $Na^+$ channel is in its open state (state O in the above model), $V$ is in mV, $E_{Na}$ = 64 mV for the conditions of these experiments, and $g_{Na}$ is given by 215 mS·cm$^{-2}$. (The maximum peak inward current amplitude of the model with a holding potential of −60 mV is 1.5 mA·cm$^{-2}$, which occurs with a step potential to +5 mV.)

### *Revised model of $I_K$*

The potassium ion current $I_K$ in the Hodgkin and Huxley (1952d) model is given by $I_K = g_K n(V, t)^4 (V - E_K)$, where $g_K$ is a constant, $E_K$ is the potassium ion equilibrium potential, and $n$ is the solution to the first order equation $dn/dt = -(\alpha_n + \beta_n)n + \alpha_n$, where $\alpha_n$ and $\beta_n$ are as given by the HH model (see APPENDIX). For a depolarizing step from rest the model predicts that $I_K = I_O[1 - \exp(-t/\tau)]^4$ with $\tau^{-1} = (\alpha_n + \beta_n)$. Fits of this equation are shown in Fig. 1 (*inset*) superimposed on experimental recordings elicited by voltage steps to −30, −10, and 10 mV from a holding potential of −70 mV. The values of $\tau$ obtained by this procedure from two different preparations are shown in the *top panel* of Fig. 1.

The primary modification in the model of the $I_K$ kinetics concerns its activation curve, which can be determined from the steady-state currents, $I_O$, in Fig. 1. Hodgkin and Huxley (1952b) carried out this procedure by normalizing their $I_O$ results by $(V - E_K)$, on the basis of their observations that the fully activated, or instantaneous, current-voltage relation for $I_K$ was a linear function of driving force. Ever since their work this aspect of $I_K$ in nerve axons has been found to be better characterized by the GHK dependence on driving

force (Binstock and Goldman 1971; Clay 1991; Clay and Shlesinger 1983; Frankenhauser 1962; Goldman 1943; Hodgkin and Katz 1949), similar to results for the $Na^+$ channel noted above. That is

$$I_K \sim V\{\exp[q(V - E_K)/kT] - 1\}/[\exp(qV/kT) - 1] \quad (3)$$

where $E_K$ is the potassium ion equilibrium potential. Consequently, steady-state measurements of $I_K$, such as the $I_O$ results in Fig. 1, should be normalized by *Eq. 3* rather than by $(V - E_K)$. Results of this analysis are shown in the *bottom panel* of Fig. 1 along with the prediction of the Hodgkin and Huxley (1952d) model (dashed line), i.e., the $n_\infty^4$ parameter, where $n_\infty = \alpha_n/(\alpha_n + \beta_n)$ with their equations for $\alpha_n$ and $\beta_n$. Both results have a threshold near $-60$ mV, but the experimental result is a much steeper function of membrane potential (especially at its foot and near its midpoint) than the HH model result. The solid curve in the *bottom panel* of Fig. 1, which was used to describe these results, also corresponds to $n_\infty^4 = [\alpha_n/(\alpha_n + \beta_n)]^4$, where $\beta_n$ has been modified as described in the APPENDIX.

The final aspect of the revised model concerns accumulation and depletion of potassium ions in the extracellular space between the axonal membrane and the glial cells surrounding the axon (Adelman et al. 1973; Frankenhauser and Hodgkin 1956). Paradoxically, these effects are not significant for strong depolarizations ($V > 0$), especially for voltage steps of brief duration, because of the nature of the dependence of the $I_K$ current-voltage relation (the GHK equation) on $K_O$ (Clay 1984). Morever, they are not significant for modest depolarizations from rest because the $K^+$ conductance is not strongly activated for these conditions. However, they are significant for voltages in the vicinity of $E_K$ following strong depolarizations (i.e., the foot of the action potential). This point is illustrated by the results in Fig. 2. The *top panel* contains measurements of $I_K$ for the potentials indicated (3-ms duration steps) and the deactivation, or ''tail'' current results on return to the holding potential ($-90$ mV) in 0 $K_O$-TTX seawater (see METHODS). The GHK equation predicts that $I_K$ should be outward at all potentials with $K_O = 0$, even $-90$ mV, as indeed was the case for the tail current after the step to $-10$ mV. [This result is shown on an expanded *y*-axis (and reduced *x*-axis) by record ''a'' in the *top right corner* of Fig. 2.] However, the tail currents following depolarizations to potentials more positive than $-10$ mV were inward with increasing inward current amplitude as the depolarization was increased, which is due in part to an increased activation of the $K^+$ conductance with potential and, in part, to the effect of potassium ion accumulation on tail current amplitude (Clay 1984). The effective potassium ion concentration in the extracellular space, $K_S$, between the axon and the glial cells was determined from the currents at the end of the depolarizing step and at the beginning of the tail current with the use of the GHK equation. (This procedure is described in detail in the legend of Fig. 2.) These results are plotted (Fig. 2, filled circles) as a function of the integral of the current during the depolarizing step (illustrated schematically by the *bottom right-hand corner inset* of Fig. 2). The rationale for this analysis is that these points should lie along a straight line if the sole mechanism by which potassium ions leave the extracellular space is passive diffusion. This conclusion appears to be appropriate for the +30, 40, and 50 mV results, but it clearly is not appropriate for the other results in Fig. 2. Indeed, the points deviate significantly below the straight line for $V = -20$ to $+20$ mV, which suggests, albeit indirectly, that another mechanism for removal of potassium ions from the extracellular space may be at work, especially when the potassium ion concentration in the Frankenhauser and Hodgkin (1956) space is <20 mM (or, alternatively, $K_S - K_O < 20$ mM, where $K_O$ is the bulk extracellular potassium concentration). These results have been modeled by

$$dK_S/dt = (\theta F)^{-1} I_K - (K_S - K_O)/\tau_1 - (K_S - K_O)/\{\tau_2[1 + (K_S - K_O)/K_d]^3\} \quad (4)$$

where $\theta$ is the width of the FH space, $F$ is the Faraday ($F = 9.65 \times 10^4$ c·mol$^{-1}$; $K_S$ and $K_O$ in units of M = mol·l$^{-1}$ = mol·10$^{-3}$ cm$^{-3}$), and $\tau_1$ is the time constant for passive diffusion of K ions from the FH space. The first two terms on the right-hand side of *Eq. 4* are the prediction of standard diffusion theory (Adelman and Fitzhugh 1975). The last term has been added to mimic the effect of the postulated uptake mechanism of K ions by the glial cells. The parameter $\tau_2$ is the apparent time constant of this effect and $K_d$ is its effective ''dissociation'' constant. Empirically it was found necessary to raise the denominator of this term to the third power, which operationally removes it from the analysis when $K_S \gg K_d$. In other words, the uptake mechanism is overwhelmed if $K_S$ is relatively large. *Equation 4* was implemented for the results in Fig. 2 by directly iterating the $I_K$ records and arbitrarily modifying the parameters $\theta$, $\tau_2$, and $K_d$ in *Eq. 4* to achieve a reasonable description of the results in the *bottom panel* of Fig. 2. (The parameter $\tau_1$ was taken as 12 ms on the basis of unpublished results by the author). The results of this analysis (represented by the open circles in Fig. 2) were $\tau_2 = 0.2$ ms, $K_d = 2$ mM, and $\theta = 11.5$ nm. The same values of these parameters were used for each open circle in Fig. 2. Only $I_K$ changed for each calculation. (Each point in Fig. 2 corresponds to a different membrane potential.) The $\theta = 11.5$ nm result is considerably less than the anatomic measurements of 40–60 nm for the width of the periaxonal space (Adelman et al. 1977; Brown and Abbott 1993). However, as Frankenhauser and Hodgkin (1956) noted, $\theta$ in equations that describe the effects of $K^+$ accumulation/depletion on electrical activity is a phenomenological parameter that does not necessarily correspond to anatomic measurements. The model described by *Eq. 4* provides a good description of the experimental results, except for $K_S - K_O < 2$ mM. In this range the uptake mechanism appears to remove K ions from the extracellular space at a greater rate than the experimental results would suggest.

The description of $I_K$ from all of the above analysis can be represented by

$$I_K(V, t) = g_K n(V, t)^4 V[e^{V/24} - (K_S/K_i)]/(e^{V/24} - 1) \quad (5)$$

where $g_K$ is the limiting slope conductance ($g_K = 62.5$ mS·cm$^{-2}$), $n(V, t)$ is as given by Hodgkin and Huxley (1952d) with the modifications in $\alpha_n$ and $\beta_n$ given in the APPENDIX, and $K_S$ is given by *Eq. 4*. Consequently, $I_K$ is determined by a system of three coupled equations: *Eq. 5* above, which gives $I_K$ directly; *Eq. 4* for $K_S$; and the first order equation for $n(V, t)$ given above and in the APPENDIX.

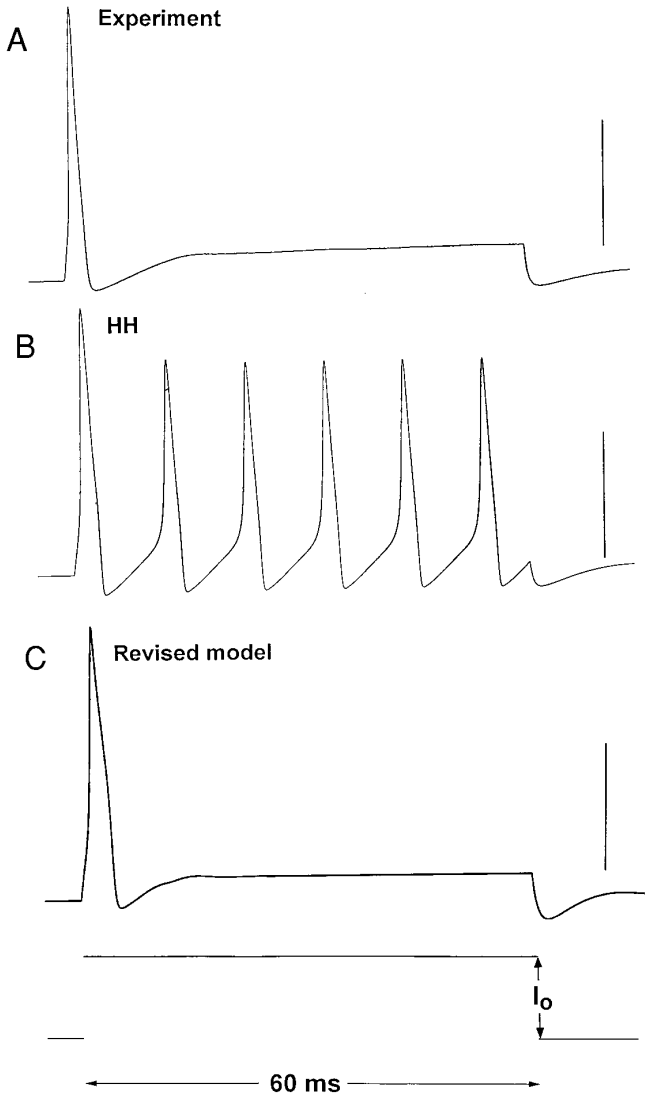


FIG. 3. Response to long duration depolarizing current pulses. *A*: axial wire stimulation of a squid giant axon with axoplasm in place. Extracellular solution was filtered seawater; $T$ = 8°C. The current pulse amplitude $I_O$ was 30 $\mu A \cdot cm^{-2}$; its duration was 60 ms. *B*: stimulation of the HH model with the same conditions as in *A*. *C*: response of the revised model to same stimulus conditions as in *A* and *B*. The calibration bar in *A*–*C* represents 50 mV (0 at top, −50 mV at bottom).

### *Squid giant axon excitability*

The response of an axon to a relatively long duration (60 ms), suprathreshold current pulse is shown in Fig. 3*A*. The pulse generated a single action potential followed by a relatively slow, depolarizing phase from the foot of the AP to a final level of −47 mV. This result was obtained from a preparation in which the axoplasm had not been removed. Similar results were obtained with intracellularly perfused axons with the standard perfusate described in METHODS. A single action potential was always obtained from the preparation for these conditions regardless of pulse amplitude or duration. The prediction of the HH model for similar conditions is shown in Fig. 3*B* (rest potential of the model = −59.9 mV). Their model generates a steady firing pattern (stable limit cycle), and this prediction is robust, occurring over a broad range of suprathreshold current pulse amplitudes. [The results illustrated in Fig. 3*A* were obtained from giant axons from *L. pealei*, the Woods Hole squid. Similar results were observed in giant axons from *L. forbesi* (E. Brown, personal communication), the preparation used by Hodgkin and Huxley (1952a–d)].

The refractory properties of the axon are further revealed by its response to trains of brief duration (1 ms) current pulses, as shown in Fig. 4*A*. In this experiment, suprathreshold current pulses were applied ~10 ms apart (same pulse amplitude for each pulse). The first pulse of the pulse train always elicited an action potential. However, the second and all subsequent pulses failed to do so. (Additional results of this nature are given in Kaplan et al. 1996.) The HH model under similar conditions exhibits a pattern of an action potential alternating with a subthreshold response (Fig. 4*B*). The model is refractory in response to the second current pulse (and also the 4th, 6th, etc.) as originally shown by Hodgkin and Huxley (1952d), but its response to a train of pulses does not match the experimental result.

A comparison of Fig. 4, *A* and *B*, also reveals a discrepancy between the HH model and the experimental preparation concerning the shape of the action potential during the latter part of repolarization, shown in greater detail in Fig. 5 for a response after a single 1-ms duration suprathreshold

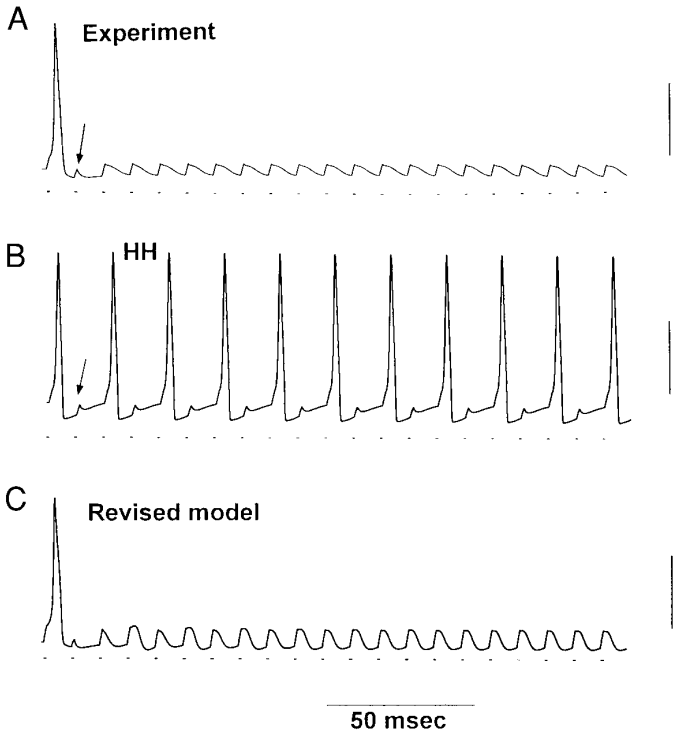


FIG. 4. Response to periodic pulse train. *A*: experimental result elicited from an intracellularly perfused axon with 1-ms duration pulses (10 $\mu A \cdot cm^{-2}$ amplitude) separated in time by 9.5 ms. (External solution, filtered seawater; standard intracellular perfusate as described in METHODS.) $T$ = 8°C. Arrow indicates the refractory response to the 2nd pulse of the train. *B*: response of HH model to the same pulse train conditions as in *A*. *C*: revised model for pulse conditions as in *A* and *B* with pulse amplitude of 14 $\mu A \cdot cm^{-2}$. (The threshold of the preparation in *A* was less than that of the model.) The vertical calibration bars in *A*–*C* represent 50 mV (as in Fig. 3). The times of application of the pulses are indicated below the traces in *A*–*C*.

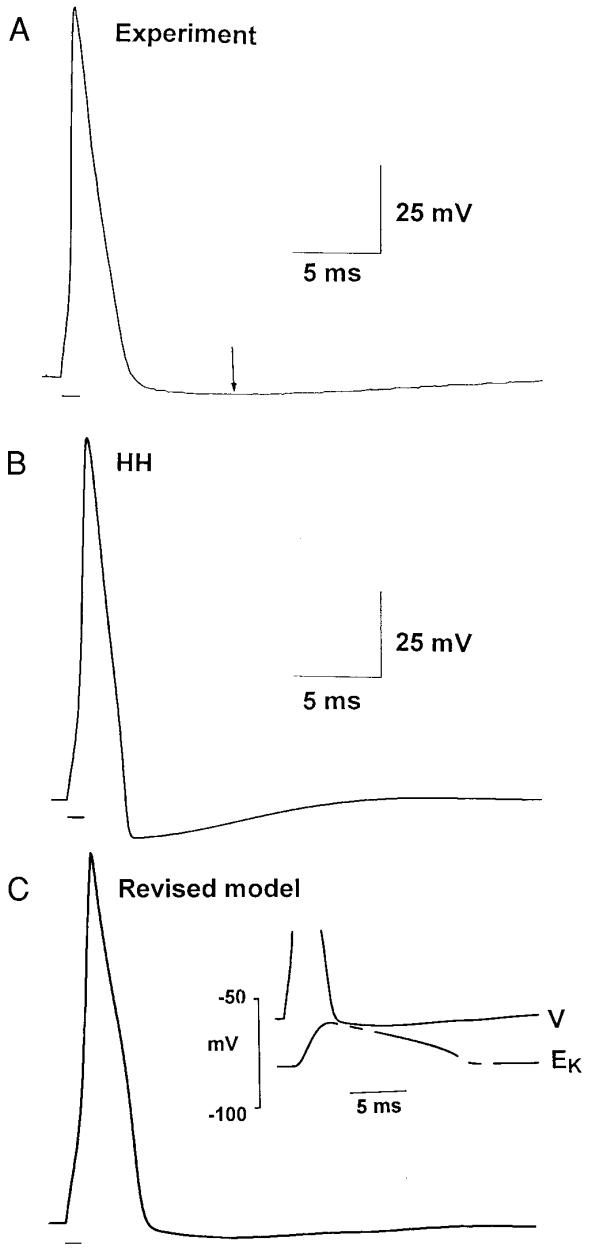


FIG. 5. Response to a single brief duration pulse. *A*: action potential elicted by a 1-ms duration pulse 40 $\mu A \cdot cm^{-2}$ in amplitude from an intracellulary perfused axon (standard perfusate) in filtered seawater. Arrow indicates the maximum afterhyperpolarization of the response. *B–C*: responses of the HH and revised models. Same pulse conditions as in *A*. The *inset* of *C* indicates the changes in the potassium ion equilibrium potential $E_K$ during the action potential of the revised model because of $K^+$ accumulation in the periaxonal space (see RESULTS). Calibrations in *C* are the same as in *A–B*. (Resting potential of the revised model is −59.4 mV). Top of the vertical calibration in *A* and *B* represents 0 mV. Small horizontal bar below each response in *A–C* represents time of pulse application.

pulse. In particular, the experimentally recorded hyperpolarizing afterpotential (Fig. 5*A*) lasts significantly longer than in the HH model (Fig. 5*B*), as indicated by the arrow in Fig. 5*A*. Similar results have been reported recently by Inoue et al. (1997) for giant axons from *Sepioteuthis*.

As shown in the following sections, modifications of the potassium ion current $I_K$ are a significant feature of the revised model of squid giant axon electrical properties. The model can be tested by removing extracellular potassium as illustrated in Fig. 6. The action potential in Fig. 6*A* was obtained with ASW as the extracellular solution (see METHODS). The resting potential of this axon was −62 mV, which is representative of the results in this study (range −65 to −55 mV) and the maximum hyperpolarizing afterpotential was −68 mV. The corresponding results for 0 $K^+$ SW (Fig. 6*B*; same preparation as in Fig. 6*A*) were resting potential, −72 mV, and maximum hyperpolarizing afterpotential, −89 mV. (Results similar to Fig. 6, *A* and *B*, were obtained with or without 50 mM $F^-$ in the intracellular perfusate, which suggests that the pump current is not a significant factor in this analysis.) The traces in Fig. 6, *C* and *D*, are the corresponding predictions of the revised model. The HH model cannot be compared with these results because the potassium ion equilibrium $E_K$ is undefined for 0 $K_O$, and $I_K$ in the HH model is directly proportional to $(V - E_K)$

### *Simulations of membrane excitability with the revised model*

Simulations with the revised model are illustrated in Figs. 3–9. The parameters of the model were the same for each simulation except for $\theta$, the effective width of space between the axon and the glial cells surrounding the axon. The potential of the afterhyperpolarizaton of the action potential varied from axon to axon (range −62 to −71 mV), which was attributed in the model to variations in accumulation/depletion through the parameter $\theta$. Specifically, $\theta$ = 11.5 (Fig. 2), 20 (Fig. 3*C*), 11 (Figs. 4*C* and 5*C*), 12 (Figs. 6, *C* and *D*), and 14 nm (Figs. 7*B*, 8*B*, and 9). The temperature was 8°C for all results except for Fig. 6, *A* and *B*, for which $T$ = 10°C. All $I_K$ and $I_{Na}$ gating parameters were scaled by a factor of 1.2 in the simulations in Fig. 6, *C* and *D*, to account for the change in $T$. Moreover, $K_O$, the extracellular potassium ion concentration in the model, was changed from 10 mM in Fig. 6*C* to 0 mM in Fig. 6*D* to match the corresponding experimental conditions in Fig. 6, *A* and *B*.

### *Shape of the action potential*

A comparison of the shape of the action potential of the model for a single depolarizing current pulse with the corresponding experimental result is given in Fig. 5, *C* and *A*, respectively. The resting potential of the model is −59.5 mV, as compared with −61 mV for the experimental preparation in Fig. 5*A*. The maximum hyperpolarizing afterpotential of the model and the experimental result are −63 and −66 mV, respectively. The latter result is 17 mV positive to $E_K$ because of $K^+$ accumulation, which reaches a maximum of 11 mM ($K_S$ = 21 mM) during the simulation in Fig. 5*C*. The time course of changes in $E_K$ during the response is illustrated by the dashed line in Fig. 5*C* (*inset*). This result, i.e., ion accumulation during a single action potential, together with the activation of $K^+$ conductance that persists after the action potential (Hodgkin and Huxley 1952d), provides a mechansim for the relatively long time that the model takes to reach its maximum hyperpolarizing afterpotential.

### *Latency to sustained depolarizing current and periodic pulse trains*

The model predicts a single action potential in response to a sustained depolarizing current pulse as illustrated in Fig.

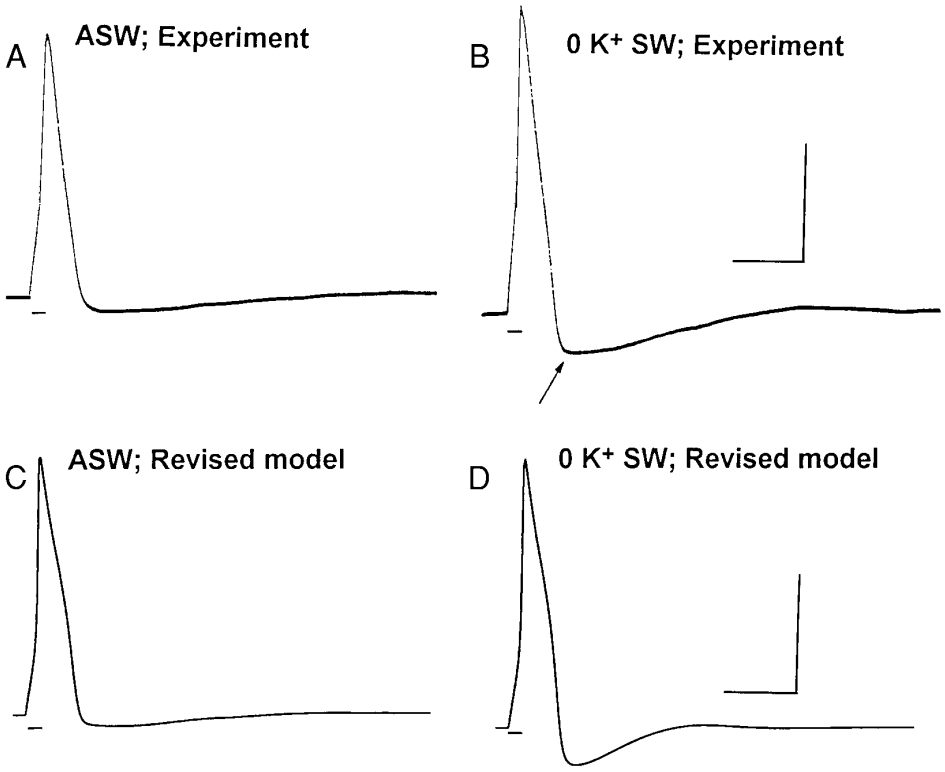


FIG. 6. Action-potential response after removal of $K_O$. *A*: action potential from an intracellularly perfused axon (standard perfusate, artificial seawater as the external solution). $T = 10$°C. *B*: response of same preparation as in *A* with 0 $K^+$ SW. Arrow illustrates the significant increase in the maximum afterhyperpolarization of the response relative to *A*. *C* and *D*: responses of the revised model with $K_O = 10$ and 0 mM, respectively. All $I_K$ and $I_{Na}$ gating parameters ($\alpha_n$ and $\beta_n$ for $I_K$, $a$, $b$, $c$, $d$, $f$, $g$, $i$, $j$, $y$, and $z$ for $I_{Na}$) were multiplied by a factor of 1.2 in these simulations to account for the change in temperature for these results ($T = 10$°C, as opposed to $T = 8$°C for all other results). Same pulse conditions in *A*–*D*. Pulse amplitude 40 $\mu A \cdot cm^{-2}$; pulse duration 1 ms. The times of pulse application are indicated under the action potential in each panel. The calibrations are 5 ms and 50 mV, respectively.

3*C*. A similar result was obtained even for very strong pulse amplitudes (100 $\mu A \cdot cm^2$). The ionic mechanisms underlying this result are not clear cut. A similar result (not shown) could also be obtained with the HH model description of $I_{Na}$ and the revised model of $I_K$ or, alternatively, with the HH model of $I_K$ and the revised model of $I_{Na}$. By contrast the response of the model to a train of pulses (Fig. 4*C*) appeared to require the Vandenberg and Bezanilla (1991b) model of $I_{Na}$. A similar result could not be obtained with the HH model of $I_{Na}$ (simulations not shown). The mechanism underlying the latency of the model to repetitive, brief duration current pulses is shown in the following sections.

### *$K_O$ removal*

The effects of $K_O$ removal on the action potential in the model are shown in Fig. 6, *C* and *D*. The resting potential of the model was hyperpolarized by only 1.7 mV when $K_O$ was set equal to 0, as compared with a 10-mV hyperpolarization in the experimental preparation in Fig. 6, *A* and *B*. The difference in these results is probably attributable to the background, or leak conductance, that is carried in part by potassium ions (Chang 1986; Clay 1988). (The leak component was not changed in the simulations in Fig. 6, *C* and *D*.) The maximum overshoot

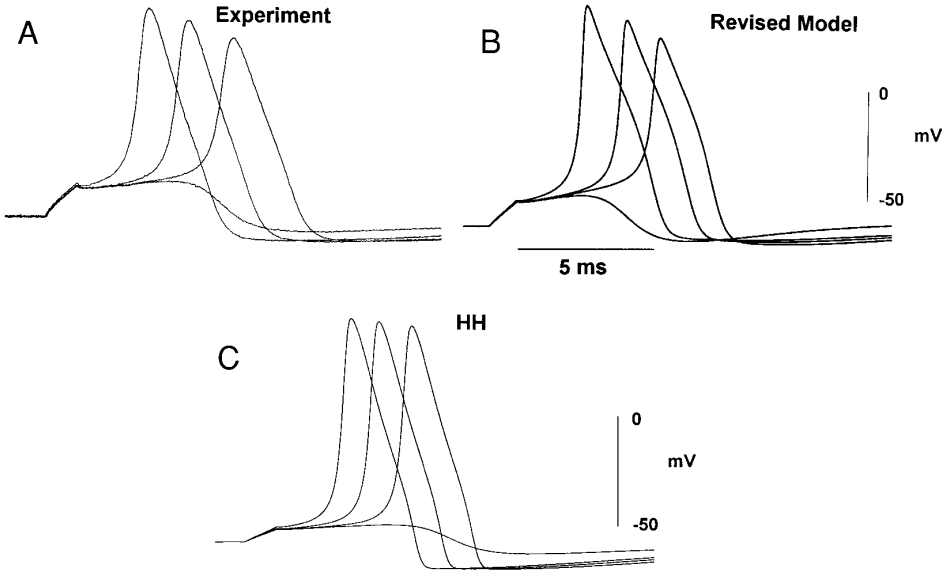


FIG. 7. Responses to near-threshold stimuli. *A*: responses of an axon to 1-ms duration pulses of amplitude 15, 14, 13.9, and 13.8 $\mu A \cdot cm^{-2}$. The latter elicited a subthreshold response, the other 3 pulses elicted action potentials with latency increasing as pulse amplitude was decreased. *B*: near-threshold results from the revised model with 14, 13.1, 13, and 12.95 $\mu A \cdot cm^{-2}$ amplitude pulses. *C*: near-threshold results from the Hodgkin and Huxley (1952d) model with 8, 7.2, 6.9, and 6.8 $\mu A \cdot cm^{-2}$ amplitude pulses.

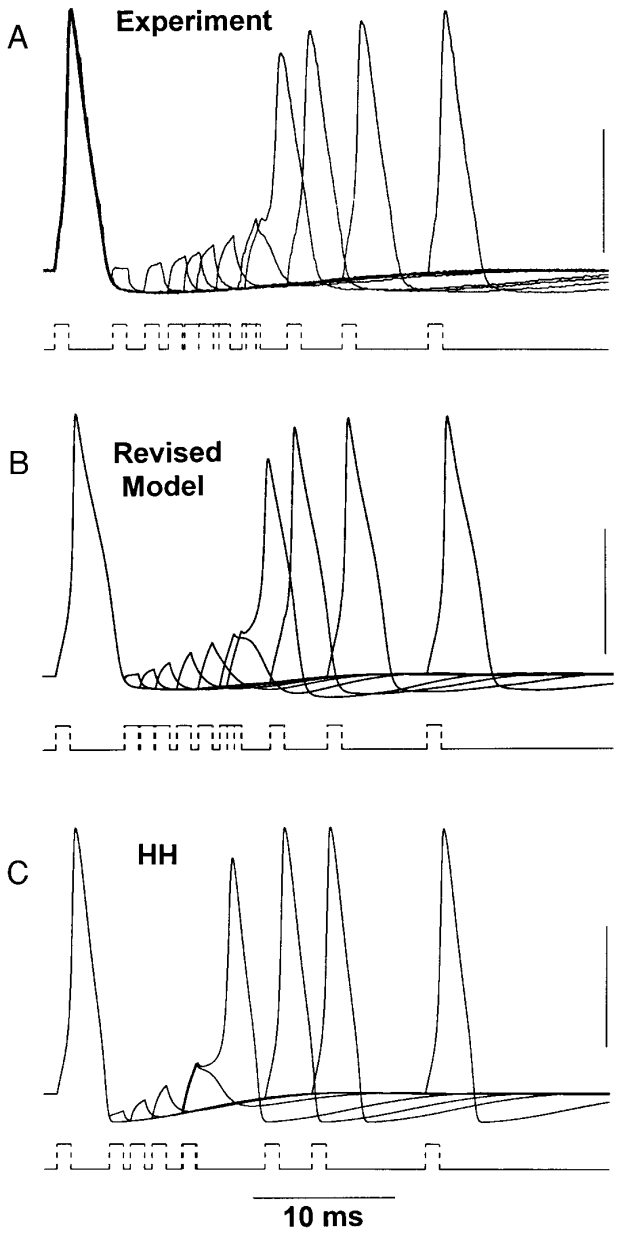


FIG. 8. Action-potential latency. For these results a 2 pulse protocol was used with variable times between the 2 pulses between 5 and 28 ms. Pulse duration was 1 ms, pulse amplitude was 30 $\mu A \cdot cm^{-2}$. The rest interval between each 2 pulse sequence was 2 s. *A*: superimposed responses of an experimental preparation to several 2 pulse stimuli. The times of pulse delivery are shown below the experimental traces. *B* and *C*: simulations of the revised and HH models, respectively, for pulse conditions that were similar to those in *A*. Pulse amplitude = 30 $\mu A \cdot cm^{-2}$. Times of pulse delivery are indicated below each panel; bar to the *right* of each panel represents 50 mV. Top of the bar is 0; bottom is −50 mV

potential in the model was increased when $K_O = 0$, because of the partial removal of $g_{Na}$ inactivation that occurs when rest potential is hyperpolarized. The maximum hyperpolarizing afterpotential of the action potential of the model with $K_O = 0$ is −77 mV as compared with −89 mV in the corresponding experimental result in Fig. 6*B*. The difference between these results would be less if the effect of potassium ion removal on leak conductance were taken into account in the model.

*Action-potential threshold*

One aspect of nerve excitability that any model must describe is action-potential threshold. These results are illustrated in Fig. 7. The experimental records in Fig. 7*A* are the responses of an axon to four different near-threshold current stimuli, each 1 ms in duration. The experimental responses clearly are not ''all-or-none.'' That is, the maximum amplitude of the response is a function of latency. Moreover, the response amplitude is a continuous (graded) function of stimulus intensity (Cole et al. 1970). This feature is usually difficult to observe experimentally because of membrane noise, although the records in Fig. 7*A* are clearly suggestive of this result. Near threshold simulations from the HH model are shown in Fig. 7*C*. These results also show a slight ''gradedness,'' although the effect is much less apparent than in the experimental results. Indeed, the stimulus intensity in the vicinity of threshold must be varied by 1 part in $10^{12}$ in the HH model to see the continuous nature of the response of the model (Clay 1977; Fitzhugh and Antosiewicz 1959). The revised model (Fig. 7*B*) provides a more faithful description of the experimental results in Fig. 7*A*, in particular the gradedness of the action-potential response to brief duration current pulses.

*Action-potential latency*

The results in Figs. 3 and 4 illustrate the relative latency of the revised model and the experimental preparation. They also suggest that the discrepancies between the axon and the HH model may be summarized by saying that the latter significantly underestimates the latency of the preparation

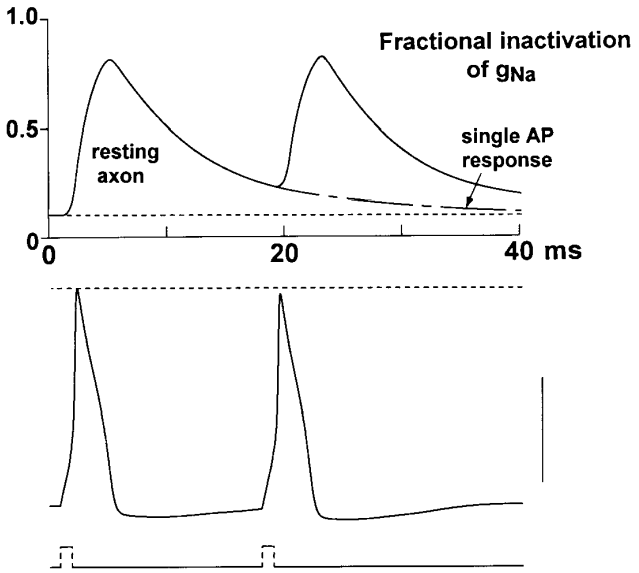


FIG. 9. Underlying mechanism of action-potential latency. *Bottom panel* was taken from Fig. 8*B* with 19 ms between current pulses (shown below the voltage trace); pulse amplitude 30 $\mu A \cdot cm^{-2}$. The second action potential has not recovered its full amplitude, as indicated by the dashed line above the action potentials. (Bar to the *right* represents 50 mV, as in Fig. 8.) The solid line in the *top panel* represents the summed probability that any single $Na^+$ channel was in any 1 of 3 inactivated states of the Vandenberg and Bezanilla (1991b) model of $I_{Na}$ gating, i.e., I, $I_4$, or $I_5$ during the simulation. roken line is the corresponding result when only a single pulse was used.

following a single action potential. This effect is shown more directly in Fig. 8. The results in Fig. 8*A* are superimposed responses of an experimental preparation to two 1-ms duration suprathreshold current pulses separated in time from between 4 and 27 ms. (The rest interval between each 2 pulse sequence was 2 s.) The preparation recovered relatively gradually from the action potential elicited by the first pulse in the two pulse protocol with a latency of ~14 ms, and the latency for the action potential to full recovery of its maximum amplitude was ~20 ms. These results were well described by the revised model (Fig. 8*B*). The HH model has approximately the same latency as the axon, although the action-potential response to the second pulse was a relatively abrupt function of the time interval between the two pulses. Furthermore, the second action potential recovered its full amplitude abruptly as the time interval between the two pulses was increased. In other words the simulations in Fig. 8*C* illustrate an approximate all-or-none recovery of the action potential as the time interval between the two pulses was increased similar to the apparent all-or-none response to a single current pulse as pulse amplitude was increased (Fig. 7*C*).

The mechanism underlying the results in Fig. 8, *A* and *B*, is illustrated in Fig. 9. The *bottom panel* of this simulation is the same as in Fig. 8*B* with a 19-ms time interval between current pulses (shown below the voltage waveform). The second response in this waveform has not quite fully recovered its maximum amplitude, as indicated by the dashed line above the action potentials. The traces in the *top panel* of Fig. 9 illustrate $g_{Na}$ inactivation during the simulation, i.e., the probability that any single sodium channel is in any one of its three inactivated states (I, $I_4$, or $I_5$) of the Vandenberg and Bezanilla (1991b) model. These results demonstrate that the model requires a long time relative to action-potential duration to return to the steady-state level of inactivation. This feature together with the relatively negative activation of $I_K$ are the primary determinants of action-potential latency in the model.

## DISCUSSION

In their original work Hodgkin and Huxley (1952a–b) demonstrated that $Na^+$ and $K^+$ have separate and distinct conductance pathways across an excitable membrane and that a mathematical description of the kinetics of these conductances could replicate an action potential and many other features of membrane excitability. Nothing in this report diminishes the significance of their work. Their model does have several shortcomings for squid giant axon electrophysiology that they realized, and that were also noted by Hodgkin (1964) in his 1961 Sherrington Lecture (in particular the results in Fig. 3). Other giant axons do fire repetitively in response to a sustained current stimulus, such as those from crustacean walking legs (Connor 1975; Hodgkin 1948). The HH model would appear to be better suited for these preparations than it is for the squid giant axon.

The refractoriness noted in RESULTS is consistent with the role that the giant axon plays in squid behavior. Squid have at least two jet-propelled escape modes: *1*) a short latency or startle response in which the giant axon fires an action potential only once and *2*) a delayed response in which it typically fires once, twice, or not at all (Otis and Gilly 1990). A repetitive train of action potentials does not appear to be involved in either of these responses. A corollary to these results is the observation in these experiments that an action potential was not elicited capriciously from the nerve. A definitive stimulus, such as a current jump, was required. For example, a current ramp did not generate an action potential unless the membrane potential was rapidly depolarized from −60 to approximately −50 mV within only a few ms, and even then the amplitude of the response was significantly less than the response elicted from the same preparation with a current jump (results not shown). A slower ramp did not elicit an action potential. Under these conditions, the membrane potential essentially followed the ramp until it reached approximately −45 mV. The preparation could not be readily depolarized beyond this point in steady-state, current-clamp conditions, probably because of the steep activation of $I_K$ in this potential range (Fig. 1).

A significant aspect of the analysis given above concerns the role of $K^+$ accumulation/depletion in the periaxonal space. In particular, the result in Fig. 5*C* suggests that the potassium ion equilibrium potential $E_K$ just outside the axon is depolarized by ~15–20 mV near the foot of an action potential. Accumulation/depletion effects have been reported elsewhere. In particular, Belluzzi et al. (1985) observed $K^+$ accumulation in rat sympathetic neurons at levels in the 20–30 mM range during activation of the delayed rectifier similar to the results reported here for squid axons. Also, Dubois (1981) has estimated $K^+$ accumulation outside nodes of Ranvier during voltage-clamp steps. A novel feature (for squid) of the description of the accumulation/depletion process in the revised model given above is the uptake mechanism of potassium ions by the glial cells that surround the axon. Buffering of extracellular potassium ion concentration by glial cells in the CNS was originally proposed by Orkland et al. (1966). Elucidation of this process in the squid giant axon preparation, if it indeed occurs, will require further experiments.

## APPENDIX

### *HH Model*

The Hodgkin and Huxley (1952d) model is described as follows

$$C\mathrm{d}V/\mathrm{d}t + (I_K + I_{Na} + I_L + I_{stim}) = 0 \qquad (A1)$$

where $V$ is membrane potential in mV, $t$ is time in ms, $C$ is the specific membrane capacitance ($C = 1\ \mu\mathrm{F}\cdot\mathrm{m}^{-2}$), $I_{stim}$ is the stimulus current ($\mu\mathrm{A}\cdot\mathrm{cm}^{-2}$), and

$$I_K = g_K n(V, t)^4 (V - E_K); \quad I_{Na} = g_{Na} m(V, t)^3 h(V, t)(V - E_{Na});$$

$$I_L = g_L (V - E_L) \qquad (A2)$$

with $g_K = 36\ \mathrm{mS}\cdot\mathrm{cm}^{-2}$; $g_{Na} = 120\ \mathrm{mS}\cdot\mathrm{cm}^{-2}$; $g_L = 0.3\ \mathrm{mS}\cdot\mathrm{cm}^{-2}$; $E_K = -72$ mV; $E_{Na} = 55$ mV; $E_L = -49$ mV; and $n$, $m$, and $h$ are given by $\mathrm{d}x/\mathrm{d}t = -(\alpha_x + \beta_x)x + \alpha_x$, where $x$ is $n$, $m$, or $h$, respectively; and $\alpha_n = -0.01(V + 50)/(\exp(-0.1(V + 50)) - 1)$; $\beta_n = 0.125\ \exp(-(V + 60)/80)$; $\alpha_m = -0.1(V + 35)/(\exp(-0.1(V + 35)) - 1)$; $\beta_m = 4\ \exp(-(V + 60)/18)$; $\alpha_h = 0.07\ \exp(-(V + 60)/20)$; and $\beta_h = 1/(\exp(-0.1(V + 30)) + 1)$. All $\alpha_x$ and $\beta_x$ are in units of $\mathrm{ms}^{-1}$. (The rest potential of the model is −59.9 mV.)

### *Revised model*

The revised model is given by *Eq. A1* as in the HH model. (Rest potential of the model is −59.5 mV.) The $I_L$ component is given as in the HH model. The $I_K$ component is given by

$$I_K = g_K n(V, t)^4 V[\exp(V/24) - K_S(t)/K_i]/[\exp(V/24) - 1] \quad (A3)$$

where $g_K = 62.5\ mS \cdot cm^{-2}$, $V$ is in mV, $t$ is in ms, $n(V, t)$ is as given by the HH model except that $\beta_n = 0.1 \exp[-(V + 60)/25]\ ms^{-1}$ [$\alpha_n$ is unchanged], $K_i$ is the intracellular potassium ion concentration ($K_i$ = 300 mM), and $K_S(t)$ is the potassium concentration in the extracellular space between the axonal membrane and the glial cells surrounding the axon. This parameter depends on time as given by

$$dK_S/dt = (F\theta)^{-1} I_K - (K_S - K_O)\tau_1^{-1} - (K_S - K_O)/[\tau_2(1 + (K_S - K_O)/K_d]^3 \quad (A4)$$

where $F$ is the Faraday ($F = 9.65 \times 10^4\ c \cdot mol^{-1}$), $\theta$ is the width of the periaxonal space, $\tau_1$ is the time constant for clearance of excess $K^+$ from the space, $K_d$ is the effective dissociation constant for removal of excess $K^+$ by the glial cells, $\tau_2$ is the time constant of this effect, and $K_O$ is the bathing potassium ion concentration ($K_O$ = 10 mM for Figs. 3, 4, 5, 6*A*, 6*C*, 7, 8, and 9; $K_O$ = 0 for Figs. 2 and 6, *B* and *D*). For all simulations $\tau_1$ = 12 ms, $\tau_2$ = 0.2 ms, and $K_d$ = 2 mM. All concentrations are in units of mM, which is the same as $mmol \cdot l^{-1}$ or $mmol \cdot 10^{-3}\ cm^{-3}$. Consequently, the first term on the right-hand side of *Eq. A4* should be multiplied by a factor of $10^{-3}$ for dimensional consistency. That is, $(F\theta)^{-1} \rightarrow 10^{-3}(F\theta)^{-1}$, or $0.104 \times 10^{-7}\ \theta^{-1}$ with $\theta$ in cm, or $0.104\ \theta^{-1}$ with $\theta$ in nm. The latter parameter is 11.5 (Fig. 2), 20 (Fig. 3*C*), 11 (Figs. 4*C* and 5*C*), 12 (Fig. 6, *C* and *D*), and 14 nm (Figs. 7*B*, 8*B*, and 9). (As noted in RESULTS, the observed variability of the maximum afterhyperpolarization of the action potential is accounted for in the model by altering $\theta$.)

The $I_{Na}$ component is given by $I_{Na} = g_{Na} P_O V\{\exp[(V - E_{Na})/24] - 1\}/\{[\exp(V/24) - 1][1 + 0.4 \exp(-0.38V/24)]\}$, with $g_{Na} = 215\ mS \cdot cm^{-2}$, $E_{Na}$ = 64 mV, and $P_O$ is the probability that any given $Na^+$ channel is in the open state (state O) of the Vandenberg and Bezanilla (1991b) model. The latter quantity is determined by the following set of equations (which follow directly from the state diagram given in RESULTS)

$$dC_2/dt = y - (2y + z)C_2 + (z - y)C_3 - y(C_4 + C_5 + I + I_4 + I_5 + O) \quad (A5)$$

$$dC_3/dt = yC_2 - (y + z)C_3 + zC_4 \quad (A6)$$

$$dC_4/dt = yC_3 - (a + z + g)C_4 + bC_5 + jI_4 \quad (A7)$$

$$dC_5/dt = aC_4 - (b + c)C_5 + dO \quad (A8)$$

$$dI/dt = -(d + i)I + cI_5 + fO \quad (A9)$$

$$dI_4/dt = gC_4 - (j + a)I_4 + bI_5 \quad (A10)$$

$$dI_5/dt = dI + aI_4 - (b + c)I_5 \quad (A11)$$

$$dO/dt = cC_5 + iI - (d + f)O \quad (A12)$$

$$C_1 = 1 - (C_2 + C_3 + C_4 + C_5 + I + I_4 + I_5 + O) \quad (A13)$$

with (in $ms^{-1}$) $a = 7.55 \exp[0.017(V - 10)]$, $b = 5.6 \exp[-0.00017(V - 10)]$, $c = 21.0 \exp[0.06(V - 10)]$, $d = 1.8 \exp[-0.02(V - 10)]$, $f = 0.56 \exp[0.00004(V - 10)]$, $g = \exp[0.00004(V - 10)]$, $i = 0.0052 \exp[-0.038(V - 10)]$, $j = 0.009 \exp[-0.038(V - 10)]$, $y = 22.0 \exp[0.014(V - 10)]$, and $z = 1.26 \exp[-0.048(V - 10)]$. All of these rate parameters have been multiplied by a factor of 1.3 to account for the temperature difference between these experiments ($T$ = 8°C) and those of Vandenberg and Bezanilla (1991a,b) for which $T$ = 5°C. Moreover, the rate parameters of the model have been shifted rightward by 10 mV along the voltage axis because the model was devised for conditions in which the external solution was free of divalent cations, whereas seawater contains 10 mM $Ca^{2+}$ and 50 mM $Mg^{2+}$. The difference between the two condtions can be accounted for by a 10 mV rightward shift of all $I_{Na}$ gating parameters along the voltage axis (Vandenberg and Bezanilla 1991a).

Address for reprint requests: National Institutes of Health, Bldg. 36, Rm. 2C02, Bethesda, MD 20892.

Received 2 July 1997; accepted in final form 11 May 1998.

## REFERENCES


ADELMAN, W. J., JR. AND FITZHUGH, R. Solutions of the Hodgkin-Huxley equations modified for potassium accumulation in a periaxonal space. *Federation Proc.* 34: 1322–1329, 1975.

ADELMAN, W. J., JR., MOSES, J., AND RICE, R. V. An anatomical basis for the resistance and capacitance in series with the excitable membrane of the squid giant axon. *J. Neurocytol.* 6: 621–646, 1977.

ADELMAN, W. J., JR., PALTI, Y., AND SENFT, J. P. Potassium ion accumulation in a periaxonal space and its effects on the measurement of membrane potassium ion conductance. *J. Membr. Biol.* 13: 387–410, 1973.

ARMSTRONG, C. M. AND BEZANILLA, F. Inactivation of the sodium channel. II. Gating current experiments. *J. Gen. Physiol.* 70: 567–590, 1977.

BELLUZZI, O., SACCHI, O., AND WANKE, E. Identification of delayed rectifier potassium and calcium currents in the rat sympathetic neurone under voltage clamp. *J. Physiol. (Lond.)* 358: 109–129, 1985.

BEZANILLA, F. AND ARMSTRONG, C. M. Inactivation of the sodium channel. I. Sodium current experiments. *J. Gen. Physiol.* 70: 549–566, 1977.

BINSTOCK, L. AND GOLDMAN, L. Rectification in instantaneous potassium current-voltage relations in *Myxicola* giant axons. *J. Physiol. (Lond.)* 217: 517–531, 1971.

BROWN, E. R. AND ABBOTT, N. J. Ultrastructure and permeability of the Schwann cell layer surrounding the giant axon of the squid. *J. Neurocytol.* 22: 283–298, 1993.

CHANG, D. Is the K permeability of the resting membrane controlled by the excitable K channel? *Biophys. J.* 50: 1095–1100, 1986.

CLAY, J. R. Monte Carlo simulation of membrane noise: an analysis of fluctuations in graded excitation of nerve membrane. *J. Theor. Biol.* 175: 257–262, 1977.

CLAY, J. R. Potassium channel kinetics in squid axons with elevated levels of external potassium concentration. *Biophys. J.* 45: 481–485, 1984.

CLAY, J. R. On the relationship between resting potential and the delayed rectifier in squid axons. *Biophys. J.* 54: 969–970, 1988.

CLAY, J. R. A paradox concerning ion permeation of the delayed rectifier potassium ion channel in squid giant axons. *J. Physiol. (Lond.)* 444: 499–511, 1991.

CLAY, J. R. A simple model of $K^+$ channel activation in nerve membrane. *J. Theor. Biol.* 175: 257–262, 1995.

CLAY, J. R. AND SHLESINGER, M. F. Effects of external cesium and rubidium on outward potassium currents in squid axons. *Biophys. J.* 42: 43–53, 1983.

COLE, K. S., GUTTMAN, R., AND BEZANILLA, F. Nerve membrane excitation without threshold. *Proc. Natl. Acad Sci. USA* 65: 884–891, 1970.

CONNOR, J. A. Neural repetitive firing: a comparative study of membrane properties of crustacean walking leg axons. *J. Neurophysiol.* 38: 922–932, 1975.

DUBOIS, J. M. Simultaneous changes in the equilibrium potential and potassium conductance in voltage clamped Ranvier node in the frog. *J. Physiol. (Lond.)* 318: 279–295, 1981.

FITZHUGH, R. AND ANTOSIEWICZ, H. A. Automatic computation of nerve excitation—detailed corrections and additions. *J. Soc. Indust. Appl. Math.* 7: 447–458, 1959.

FRANKENHAUSER, B. Potassium permeability in myelinated nerve fibers of *Xenopus laevis*. *J. Physiol. (Lond.)* 160: 54–61, 1962.

FRANKENHAUSER, B. AND HODGKIN, A. L. The after-effects of impulses in the giant nerve fibres of *Loligo*. *J. Physiol. (Lond.)* 131: 341–376, 1956.

FRENCH, R. J. AND WELLS, J. B. Sodium ions as blocking agents and charge carriers in the potassium channel of the squid giant axon. *J. Gen. Physiol.* 70: 707–724, 1977.

GOLDMAN, D. E. Potential, impedance, and rectification in membranes. *J. Gen. Physiol.* 27: 37–60, 1943.

HODGKIN, A. L. The local electrical changes associated with repetitive action in a nonmedullated axon. *J. Physiol. (Lond.)* 107: 165–181, 1948.

HODGKIN, A. L. *The Conduction of the Nervous Impulse*. Liverpool, UK: Liverpool Univ. Press, 1964.

HODGKIN, A. L. AND HUXLEY, A. F. Currents carried by sodium and potassium ions through the membranes of the giant axon of *Loligo*. *J. Physiol. (Lond.)* 116: 449–472, 1952a.

HODGKIN, A. L. AND HUXLEY, A. F. The components of membrane conductance in the giant axon of *Loligo*. *J. Physiol. (Lond.)* 116: 473–496, 1952b.

HODGKIN, A. L. AND HUXLEY, A. F. The dual effect of membrane potential on sodium conductance in the giant axon of *Loligo*. *J. Physiol. (Lond.)* 116: 497–506, 1952c.

HODGKIN, A. L. AND HUXLEY, A. F. A quantitative description of membrane conductance and its application to conduction and excitation in nerve. *J. Physiol. (Lond.)* 117: 500–544, 1952d.

HODGKIN, A. L. AND KATZ, B. The effect of sodium ions on the electrical activity of the giant axon of the squid. *J. Physiol. (Lond.)* 108: 37–77, 1949.

INOUE, I., TSUTSUI, K., AND BROWN, E. R. $K^+$ accumulation and $K^+$ conductance inactivation during action potential trains in giant axons of the squid *Sepiotheuthis*. *J. Physiol. (Lond.)* 500: 355–366, 1997.

KAPLAN, D. T., CLAY, J. R., MANNING, T., GLASS, L., GUEVARA, M. G., AND SHRIER, A. Subthreshold dynamics in periodically stimulated squid giant axons. *Physiol. Rev. Lett.* 76: 4074–4077, 1996.

ORKLAND, R. K., NICHOLLS, J. G., AND KUFFLER, S. W. Effects of nerve impulses on the membrane potential of glial cells in the central nervous system of amphibia. *J. Neurophysiol.* 29: 788–806, 1966.

OTIS, T. S. AND GILLY, W. F. Jet-propelled escape in the squid *Loligo opalescens*: concerted control by giant and non-giant motor axon pathways. *Proc. Natl. Acad. Sci. USA* 87: 2911–2915, 1990.

PATLAK, J. Molecular kinetics of voltage-dependent $Na^+$ channels. *Physiol. Rev.* 71: 1047–1080, 1991.

VANDENBERG, C. A. AND BEZANILLA, F. Single-channel, macroscopic, and gating currents from sodium channels in the squid giant axon. *Biophys. J.* 60: 1499–1510, 1991a.

VANDENBERG, C. A. AND BEZANILLA, F. A sodium channel gating model based on single channel, macroscopic ionic, and gating currents in the squid giant axon. *Biophys. J.* 60: 1511–1533, 1991b.

YAMAMOTO, D., YEH, J. Z., AND NARAHASHI, T. Voltage-dependent calcium block of normal and tetramethrin-modified single sodium channels. *Biophys. J.* 45: 337–344, 1984.